Canadian Conference - Pacific Conference on Earthquake Engineering 2023
Vancouver, British Columbia
June 25th – June 30th, 2023

Multi-Platform Numerical Hybrid Simulation Assessment of the Seismic Stability of the E-BRBF Systems for Tall Buildings in Vancouver

Bashar Hariri[1*], Robert Tremblay[2] and Constantin Christopoulos[3]

[1]Postdoctoral Research Fellow, Department of Civil and Mineral Engineering University of Toronto, Toronto, ON, Canada
[2]Professor, Department of Civil, Geological and Mining Engineering, Polytechnique Montreal, Montreal, QC, Canada
[3]Professor, Department of Civil and Mineral Engineering University of Toronto, Toronto, ON, Canada
[*]bashar.hariri@utoronto.ca (Corresponding Author)

ABSTRACT

This article examines the seismic stability of the E-BRBF systems used in tall building structures subjected to interface subduction earthquakes. The E-BRBF system is a buckling restrained steel braced frame with an inverted-V brace configuration in which one of the two braces is a conventional brace designed to remain elastic during strong earthquake events. At every storey, the beam and the elastic braces develop sufficient post-yielding stiffness that cancels out the negative storey shear stiffness resulting from P-delta effects, thereby ensuring the stability of the structure when responding in the nonlinear range. The global seismic stability in E-BRBFs relies heavily on the stable and predictable response of the beams under axial and flexural demands. Past numerical studies have demonstrated the adequacy of E-BRBF beams in mitigating P-delta effects in steel buildings with heights up to 40 storeys using distributed-plasticity fibre-section beam models. This article utilizes a more refined and representative beam model to numerically test the performance of a 10-storey E-BRBF under static-monotonic and dynamic response history analysis using seismic excitations representative of the seismic hazard of Vancouver, BC (i.e., Crustal, In Slab, and Subduction Interface). The assessments are conducted in standalone mode as well as hybrid simulation mode. In the hybrid mode, the first-storey beam of the E-BRBF is sub-structured in Abaqus using solid elements, and the rest of the E-BRBF frame is integrated with OpenSees using fibre-based sections. A total of 24 DOFs are transferred between the integration and the substructure modules utilizing the UT-SIM communication protocols developed at the University of Toronto. The conducted dynamic nonlinear response history analyses demonstrate an identical seismic performance to the case of numerical simulations performed using the complete OpenSees model (standalone mode). The monotonic Pushover hybrid simulations show a higher contribution from the beam to global seismic stability compared to the results obtained with the standalone mode models. The analysis also reveals that a ductile plastic hinging mechanism with no instability failure modes is obtained at extreme drifts.

Keywords: Seismic stability, P-delta effects, Numerical hybrid simulation, Post-yielding stiffness, E-BRBF

INTRODUCTION

The seismic performance of multi-storey steel buildings is highly influenced by the second-order P-delta effects [1-4]. P-delta effects introduce a storey shear force demand that reduces the strength capacity of the seismic force-resisting system (SFRS), which compromises its ability to dissipate seismic energy and thereby imposes larger storey drifts (Fig. 1a). Taller buildings are more susceptible to P-delta effects [5] as they carry more substantial gravity loads and deform in a multi-mode inelastic configuration. Past studies [6-13] have shown that P-delta effects on the inelastic seismic response of multi-storey buildings are also more pronounced under long-duration ground motions such as those generated from large magnitude interface subduction earthquakes given the large number of inelastic cyclic reversals that creates progressive drifting of the structure in one direction, which can lead to structural collapse by instability. International design codes address P-delta effects by amplifying the yielding strengths of the SFRS ductile members using a stability coefficient to substitute the strength reduction imposed by P-delta (Fig. 1b). The standards quantify the strength amplification of every storey based on the carried gravity load and the estimated drift. Design standards vary in estimating the storey drifts. In Canada for instance, the Canadian steel design standard CSA S16-19 [14] requires using the inelastic drift estimated by amplifying the first-order design drift with the ductility factor; however, AISC [15] uses the first-order design drifts directly. Although this estimation might be sufficiently accurate in single-mode deformable structures (i.e., SDOFs), several researchers argued the extension to multi-storey buildings. More specifically, Adam [3] reported that it is meaningless to estimate the inelastic drift of MDOF systems given the complicated and ground motion-dependent inelastic deformed configuration that involves higher modes. Given its insufficiency, steel design standards in North America (i.e., CSA S16 and AISC) enforce additional stability-related stringent provisions to mitigate P-delta effects, for instance, BRBFs are limited to 40 m in height. This restriction, however, contributes to reducing the uncertainty of the deformed configuration under seismic loading and limits the total carried gravity loading. Hariri and Tremblay [12, 13] furtherly evaluated the need for the CSA S16 BRBF height limitations when incorporating the strength amplification approach in mitigating P-delta effects for mid- and high-rise BRBFs. The study also extended the assessment to involve EBFs and concluded that the height restriction is crucial and needs to be extended to EBFs, a similar recommendation was also reported by Chen et al., [16].

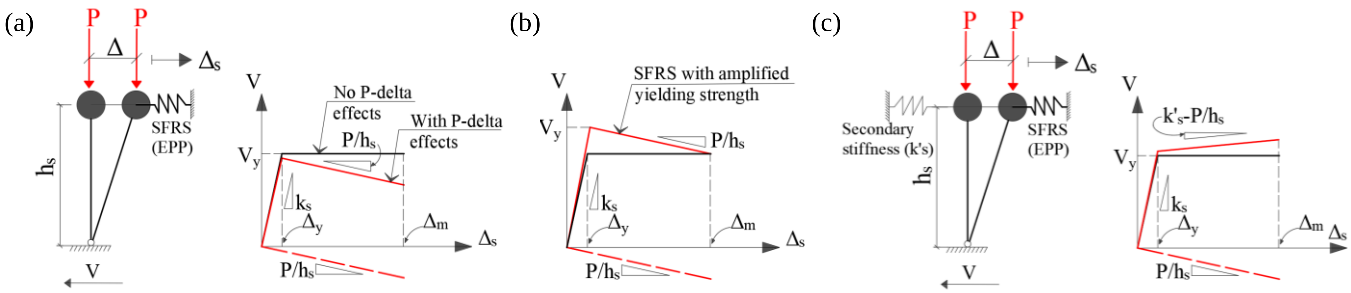

Figure 1. P-delta effects and mitigating approaches: (a) P-delta effects on EPP SDOF system, (b) Yielding strength amplification approach, (c) Incorporating secondary stiffness approach.

Another approach to mitigating P-delta effects was proposed in the literature [3, 11-13, 17-19]. The approach relies on incorporating a secondary positive post-yielding storey shear stiffness that is sufficient to cancel the negative storey shear stiffness resulting from P-delta effects, thereby ensuring the stability of the structure when responding in the nonlinear range (Fig. 1c). To assess P-delta mitigation approaches, Hariri and Tremblay [12] numerically examined the seismic stability of 10-, 20-, 30, and 40-storey Eccentrical (EBF), Buckling-restrained (BRBF) and Bolted-end friction (FBF) steel braced frames designed per the Canadian steel design standard CSA S16 using nonlinear response history analysis under three sources of seismic excitations (i.e., Crustal, In Slab, and Subduction Interface). The study considered two analysis cases when dealing with second-order geometrical nonlinearity (i.e., P-delta). The study concluded that considering the seismic component only (i.e., no P-delta effects), the SFRSs demonstrated a stable seismic performance and uniform drift distribution along buildings' heights, as well as repairable-limit residual drifts in the case of EBFs and BRBs. However, introducing the P-delta analysis and mitigating it utilizing the strength amplification approach resulted in second-order storey shear forces that disturbed the uniformity of drift distribution and induced drift concentration that led to excessive drifts and global instability, especially under subduction interface seismic excitations. Contrarily, incorporating secondary storey shear stiffness demonstrated stable seismic performance with residual and peak inter-storey drift distribution identical to the case of no P-delta analysis. The study quantified the minimum positive post-yielding stiffness essential to cancel P-delta effects using an ideal-but-fictitious source of post-yielding stiffness and concluded that post-yielding stiffness needs to be equal to the negative stiffness induced by P-delta in every storey. In addition, the post-yielding stiffness must be maintained for storey drifts adequate for the energy-dissipation process. The study quantified this drift to be 2.5% of storey height for mid-rise steel braced frames (i.e., 10- and 20-storey) and 2.0% for the high-rise (i.e., 30- and 40-storey).

Tremblay [19] proposed a steel-braced frame with the self-capability of developing post-yielding storey shear stiffness. The system is referred to here as E-FBF. E-FBF is a bolted-end friction braced frame with an inverted-V brace configuration in which one of the two braces is a conventional brace designed to remain elastic during a strong earthquake event. When the friction element slips, an unbalanced vertical force develops at the brace-to-beam connection, which imposes flexural demand on the beam and creates a positive post-yielding storey shear stiffness, as illustrated in Figure 2. The application of beam flexural stiffness as a source of secondary lateral storey shear stiffness was then extended to buckling-restrained steel braced frames (i.e., E-BRBF) [20].

The global seismic stability in E-BRBFs and E-FBFs heavily relies on a stable and predictable response of the beams under axial and flexural demand. That response can be affected by localized yielding and local instability effects resulting from residual stresses, stress concentration near gusset plate connections and geometric imperfections. Past studies [11-13, 19, 20] demonstrated the adequacy of E-BRBF and similar beam-induced secondary storey shear stiffness systems in steel buildings with heights up to 40 storeys. The assessments included response history analyses that involved subduction interface seismic excitations; however, using simplified distributed-plasticity fibre-section models in OpenSees. Although these models are adequate in capturing global behaviour, they are insufficient to capture advanced stability-related beam failures. Therefore, a comprehensive assessment of the force demand on and the cyclic response of the beams must be performed to develop proper provisions for the selection of a suitable beam section, connection details and bracing requirements. A research project has been initiated that will include quasi-static cyclic testing and hybrid seismic testing to be performed on full-scale one-storey column-brace-beam sub-assemblages. The first phase of this project consists of performing numerical hybrid simulations where the beam and brace connections at the first storey of a 10-storey E-BRBF building are represented with a detailed finite element model in Abaqus, and the rest of the structure is modelled using the OpenSees program. The hybrid simulation is performed using the UT-SIM communication protocols [21, 22] developed at the University of Toronto. The 10-storey E-BRBF structure is designed for Vancouver, BC, using the provisions of the 2020 NBC [23] and CSA S16-19 [14]. Nonlinear static incremental (pushover) analysis is performed, as well as response history analysis using an ensemble of ground motion records from crustal, sub-crustal, and interface subduction earthquakes that contribute to the seismic hazard in Vancouver.

This article presents the numerical hybrid simulation phase of the work, including a description of the model and an examination of the obtained results. A comparison with the results obtained from numerical simulations performed using a complete OpenSees model of the structure are also presented and discussed.

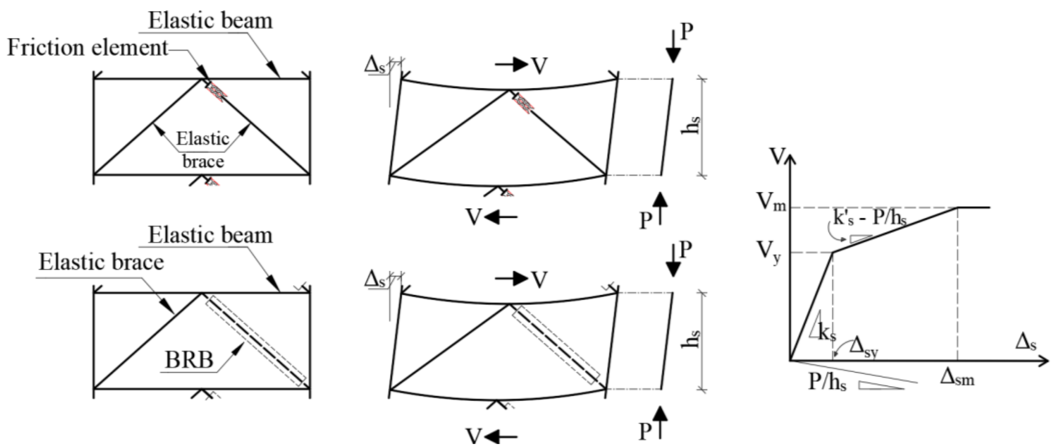

Figure 2. E-FBF and E-BRBF systems proposed by Tremblay [19].

DESIGN OF PROTOTYPE BUILDING

Description and design of the studied building

This article considers a 10-storey office steel building located in Vancouver, BC, on soil with a shear wave velocity (V_{s30}) of 400 m/s (i.e., Class C). The building is symmetric with six bays @ 9 m spans with constant storey height (4 m) except for the first floor (4.5 m). The seismic force-resisting system consists of four E-BRBFs located on the exterior column line of the building in both principal directions. The E-BRBFs are non-concentric with an inverted-V chevron bracing configuration where the beam-brace connection assembly is shifted by 2 m from the center to mobilize less flexural demand on the beam, which permits more ductile behaviour at extreme drifts. Buckling restrained braces are steel-restrained with low-strain hardening (i.e., stability-critical case [24]). Figure 3 illustrates the building layout plan, the utilized SFRS, and the design gravity loads.

Seismic design provisions

The 10-storey building is designed following the 2020 National Building Code of Canada NBC [23] and the Canadian steel design standard CSA S16-19 [14]. The SFRS design base shear is calculated based on Eq (1) as a fraction of the total seismic weight calculated using load combination of (Dead + 0.25Snow), where S represents the spectral acceleration calculated at the period T_a from the 2% in 50 years Uniform Hazard Spectrum of Vancouver, BC [25]. R_o and R_d are the ductility and the overstrength adjustment factors. I_E is the importance factor and M_v represents the base shear adjustment factor for higher modes. A minimum base shear cut-off at 2 s (V_{min}) is stipulated by NBC for the base shear calculated per Eq. (2). Since the building has no irregularity and designed respecting the response spectrum analysis, NBC permits reducing the base shear calculated using Eq. (1) by 20% when comparing with the dynamic base shear to obtain the greatest and employ it as the design base shear (V_d).

$$V = \frac{S(T_a) I_E M_v W}{R_d R_o} \geq V_{\min} \tag{1}$$

The SFRS in the considered prototype building is designed using response spectrum analysis considering 12 elastic modes. The ductility and overstrength adjustment factors are 4 and 1.2, respectively. The importance and higher mode factors are taken as

1. The design base shear to total seismic weight ratio (V_d/W) is 0.055, and the first three dynamic periods are 2.16 s, 0.77 s, 0.44 s, respectively.

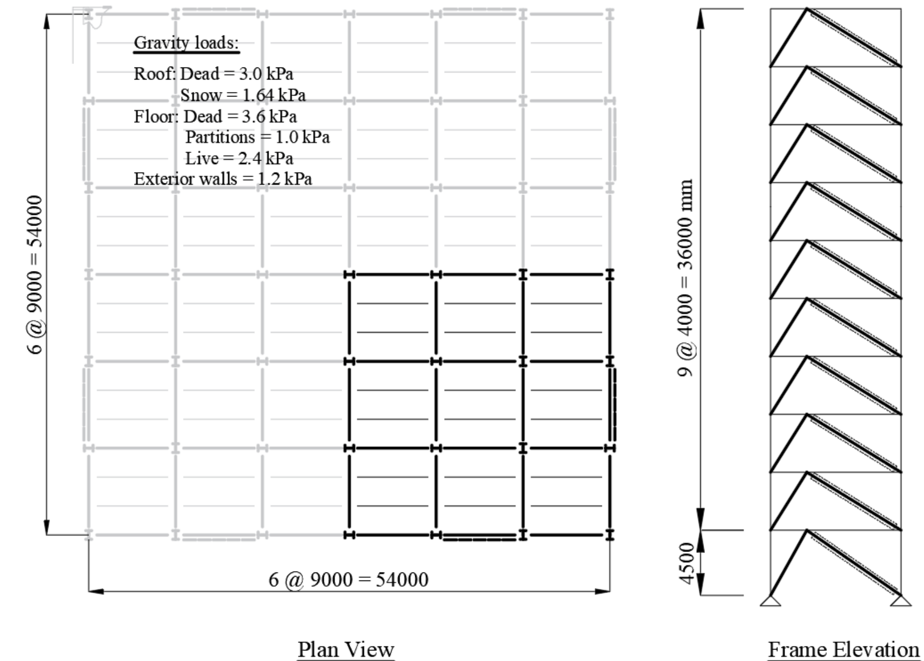

Figure 3. 10-Storey E-BRBF prototype building.

Design of E-BRB frame

The 10-storey E-BRBF is designed to develop post-yielding lateral storey shear stiffness (i.e., k'_s) equal to the negative stiffness induced by the P-delta effect (i.e., P/h_s) on a storey-by-storey basis, where h_s is the storey height and P is total storey gravity load calculated using (Dead + 0.5Live + 0.25Snow) load combination after accounting for the live load reduction considering the attributed area. The BRBs, beams, elastic braces, and columns are selected iteratively. For each iteration, the BRB core area is calculated based on the storey shear (V_y) (Fig. 4). The beam section is then selected, providing that the k'_s calculated per figure 4 falls within the 0 to 15% range exceeding the negative stiffness of P-delta (i.e., P/h_s). The cross-sectional strength, the flexural, and the lateral-flexural buckling of the beam are then verified under the axial and flexural load demands calculated based on the developed stiffness assuming a storey drift of 2.5%h_s and considering two out-of-plane flange lateral supports. The first support is located at the beam-brace intersection, and the second is at the middle of the beam's long end (Fig. 4). Once the beam's section is obtained, the elastic brace and the columns are designed for the maximum storey shear V_m (Figure 4) using capacity design. After the E-BRBF members have been selected, the base shear is re-calculated based on the new period, and the procedure is repeated until the fundamental period converges.

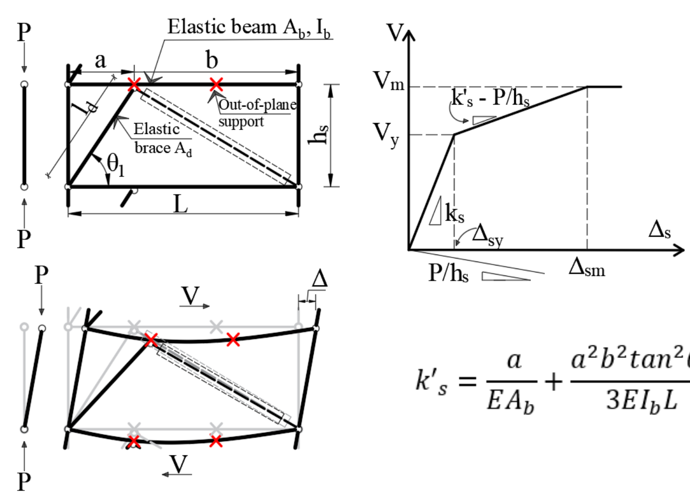

$$k'_s = \frac{a}{EA_b} + \frac{a^2 b^2 tan^2\theta_1}{3EI_b L} + \frac{l_d}{EA_d cos^2\theta_1}$$

Figure 4. E-BRBF design.

Based on the proposed E-BRBF design procedure, a *W*360x421 is selected for the E-BRBF first-storey beam (Figure 5). The developed lateral post-yielding first-storey shear stiffness (k'_s) is 9.47 kN/mm^2. The P-delta negative stiffness developed considering the gravity loads assigned to a single E-BRBF is 8.49 kN/mm^2 (i.e., k'_s /(P/h_s) = 9.47/8.49 = 1.12). The beam is designed to remain elastic for a lateral storey drift of 112.5 mm (i.e., 2.5%h_s). Based on the selected BRB core area, the first-storey E-BRBF yielding strength V_y is 2290 kN, and the maximum storey shear based on the selected beam V_m is 3260. Those values, however, exclude the isotropic and kinematic strain hardenings expected to develop by the BRB member. Amplifying the yielding strength of the BRB with a factor of 1.54 (i.e., ω.β = 1.4x1.1=1.54) gives the ultimate yielding and maximum strengths V_y and V_m as 3530 kN, 4500 kN, respectively. The ultimate maximum strength (i.e., V_m) is used in designing the remaining structural members of the E-BRBF. The selected elastic brace is *W*360x134, and the columns are *W*360x509. The gusset plate is designed concerning the maximum forces developed by the braces at V_m. The selected thickness of the gusset plate is 23 mm. The gusset is stiffened for out-of-plane buckling using 18 mm stiffeners on both sides (Figure. 5). 18 mm full-flange beam-web stiffeners are added at the locations of the out-of-plane lateral supports (to connect the lateral beams), as well as where maximum shear stresses are expected (i.e., beam end supports, and gusset plate ends).

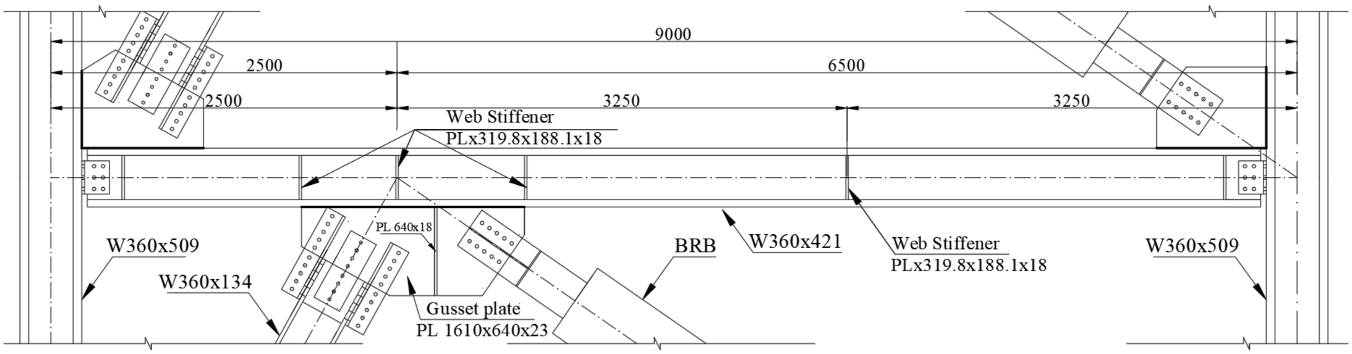

Figure 5. 10-storey E-BRBF first storey beam.

NUMERICAL MODELLING

The SFRS of the 10-storey prototype building consists of four E-BRBFs in each principal direction. Since the building is symmetrical about its principal axes, a single 10-storey E-BRBF with the building's quarter mass and quarter gravity loads is modelled. The model in the standalone mode is entirely in OpenSees, however, the hybrid mode of analysis spreads over two platforms, Abaqus [26] and OpenSees [27], where the E-BRBF's first-storey beam is modelled in the Abaqus platform (i.e., Substructure Module), while the rest of the E-BRBF structural components are modelled in OpenSees (i.e., Integration Module). Four discretized nodes, A, B, C, and D are used to connect the modules. Each node transfers three translational and three rotational DOFs, as well as three forces and three moments, forming 48 communicated signals over the local host IP address. The communication is carried out utilizing the state-of-art UT-SIM communication protocols [21, 22] developed at the University of Toronto. Figure 6a illustrates the modelling layout.

Substructure module – Hybrid analysis

The E-BRBF's first-storey beam member and stiffener plates are modelled in the Abaqus FEA programme using C3D8R-type solid elements. The gusset plate connecting the beam with the elastic brace and the BRB is modelled using a combination of two element types, the C3D8R and the C3D6, to account for the plate's chamfered edges. A992-GR50 calibrated steel parameters by Hartloper et al, [28] are utilized with a slight modification to maintain consistency with OpenSees. The modified parameters are Young's modulus and the yielding strength, and were taken as 200 GPa and 385 MPa, respectively. Initial imperfections are modelled as an initial state using a modified geometry utilizing three buckling modes scaled to satisfy the maximum CSA S16-19 imperfection tolerance (i.e., L/500). The elastic buckling modes involved lateral-flexural buckling, flange local buckling, and out-of-plane gusset buckling. The residual stresses are modelled as an initial pre-defined stress field utilizing the Galambos and Ketter pattern [29]. Beams' pinned ends are simulated using pin constrains that connect the web ends to the modules-connecting nodes A and D, as illustrated in Figure 6b. The elastic brace connecting node (i.e., node B) is constrained to the gusset bolts' nodes using a tie constraint, and the BRB connecting node (i.e., node C) is constrained to the gusset BRB bolts using a pin constraint. Gravity load based on the beam's attributed area is modelled using 10 equally-placed nodes located on the center-line of the top flange. Out-of-plane lateral support boundary conditions are assigned to both flanges at the sections indicated in the design (Fig. 6b). Figure 6b illustrates the beam's model.

Integration module – Hybrid analysis

The E-BRBF structural components excluding the first-storey beam are modelled in the OpenSees platform. The BRB elements are modelled using truss elements. The beams, elastic braces, and column are modelled using multi-element nonlinear beam-columns with initial imperfection of L/500 assigned using a sine function to the weak direction. Beams are pin constrained to the columns and columns are continuously-spliced every two storeys. Elastic braces are connected to the beam using zero length link elements with flexural properties representative of gusset plates. Zsarnóczay [30] *steel4* material with parameters calibrated per Hariri and Tremblay [24] are assigned to BRB elements. Fiber sections with Giuffre-Menegotto-Pinto *steel02* material with default parameters are assigned to beams, columns, and elastic braces. Residual stresses are applied to fiber sections using the Galambos and Ketter distribution [29]. To account for BRB end connections, the axial stiffness of the modelled truss elements is amplified by a factor of 1.5, as specified by the CoreBrace BRB design guide [31]. Gravity loads are assigned using an axially-stiff leaning column constrained to the E-BRBF using a single node X-direction translational constraint. The storey masses are lumped at storey levels and assigned to the columns. Current-step mass and stiffness proportional Rayleigh damping is assigned using parameters calculated considering the first and the third modes with a 0.03 damping coefficient.

Complete fiber-section model – Standalone analysis

The E-BRBF in the Complete fibre-section model is entirely modelled in the OpenSees platform, including the E-BRBF first-storey beam. The model is intended to run as a standalone model (i.e., non-hybrid) and represents a reference to monitor the differences in analysis results with the hybrid ones. The modelling assumptions and techniques of the integration module are extended to the standalone model.

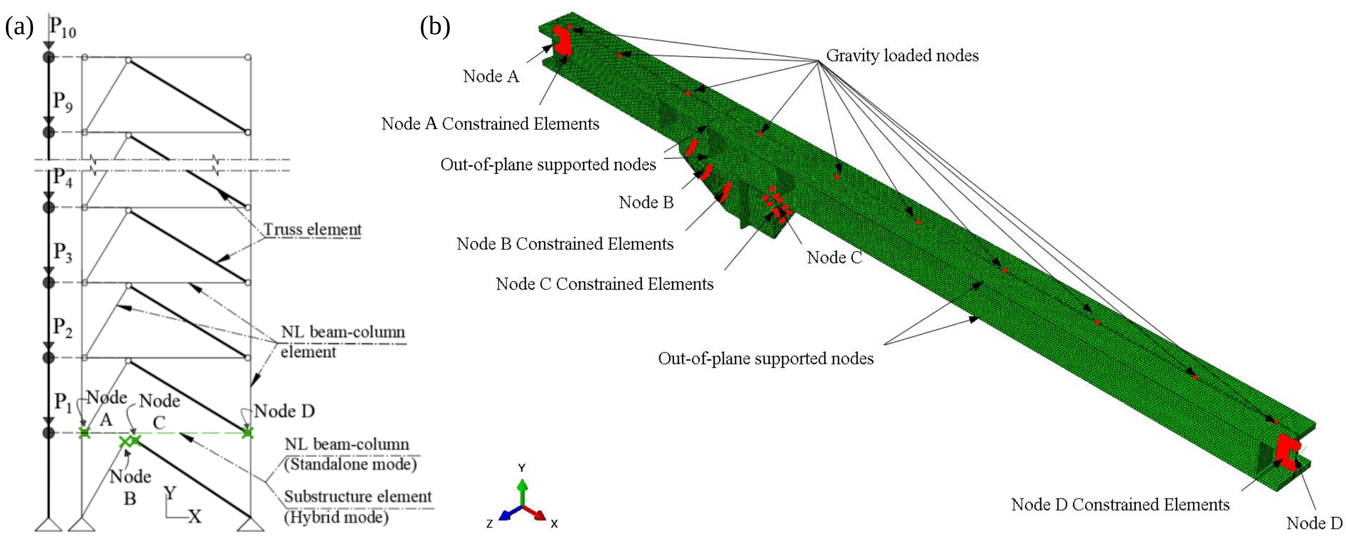

Figure 6. Modelling layout: (a) E-BRBF, (b) Sub-structured beam.

Seismic records

As part of the modelling, an ensemble of 22 historical earthquake records is developed. The records are selected and scaled using scenario-specific ranges utilizing an automated tool [32] to match the 2020 2% in 50 years Uniform Hazard Spectrum (i.e., design spectrum) of Vancouver, BC., as specified in the NBC 2020 [23]. The records are sorted in two Suites, Suite 1 involves 6 Crustal and five deep In Slab records scaled to match the short period range of the spectrum (i.e., 0.3 s to 1.2 s). Suite 2 involves 11 Subduction Interface motions, scaled to match the spectrum in the long period range (i.e., 1.2 s to 4.5 s) as de-aggregated by Halchuk et al., [33]. Figure 7 illustrates the design spectrum and considered seismic records.

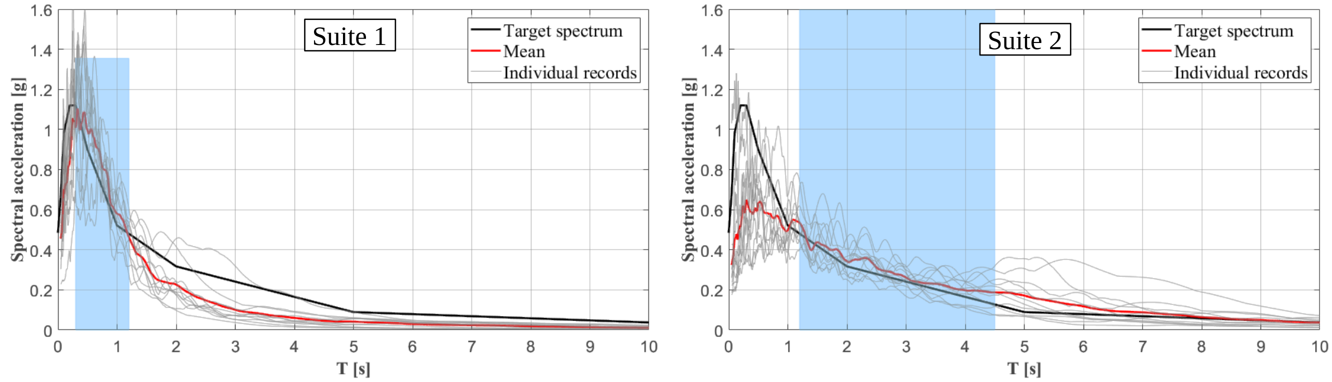

Figure 7. Design spectrum with selected / scaled historical records.

The National building code of Canada defines the Seismic Demand curve (i.e., SD curve) as the largest curve of the suites' mean response curves, and defines the maximum allowed total lateral storey drift as 2.5%h_s, where h_s is storey height.

ANALYSIS RESULTS

Pushover analysis

Figure 8a presents pushover curves under static nonlinear analysis conducted to assess the adequacy of the E-BRBF beam located at the first storey in developing the intended post-yielding stiffness and to investigate its potential failure modes under extreme loading. The analysis is performed in hybrid mode and standalone mode. Pushover curves resulting from both modes are presented in the figure under positive and negative displacement loading directions. Since the analysis aims to assess the first-storey beam, the pushover loading pattern is therefore confined to the first storey (Fig. 8a). The analysis is conducted under the following conditions to test the beam for extreme loading and eliminate other structural members from contributing to the post-yielding stiffness: 1) the columns and elastic braces are pinned at every storey. 2) Elastic-perfectly plastic material model is used for BRBF elements (i.e., no BRB strain hardening). 3) BRB material utilizes the ultimate yielding strength (i.e., beam critical loading condition).

The figure reveals that the hybrid and standalone analyses develop identical curves for drifts within the elastic deformation range of the first-storey BRB. For drifts beyond the BRB yielding and less than 2.5%h_s (i.e., design limit), the post-yielding stiffness developed by the hybrid model in the positive drift loading direction slightly exceeds the 0.12 P/h_s developed by the standalone model; however, curves remain identical in the negative direction loading drift. This behaviour is attributed to the contribution of the gusset plate stiffness developed when the plate is loaded in tension (i.e., positive drift loading direction), as the slight buckling of the plate in the negative drift loading direction voids this induced stiffness.

For drifts beyond the beam-yielding design drift (i.e., 2.5% h_s), the standalone model presents a decay in post-yielding stiffness development under loads in both directions due to the formation of a plastic hinge at the beam-brace section. In contrast, the presence of the gusset plate in the hybrid model shifts the location of the beam plastic hinging outside the extent of the plate, which allows the elastic behaviour of the beam to extend for larger drifts (Figs. 8b and 8c).

Ultimately, the hybrid and the standalone models demonstrated a ductile post-hinging behaviour for drifts up to twice the design value with no observed stability failure. More specifically, the observed failure mode was full-hinging with no local buckling, flange-gusset instability, or lateral-flexural buckling.

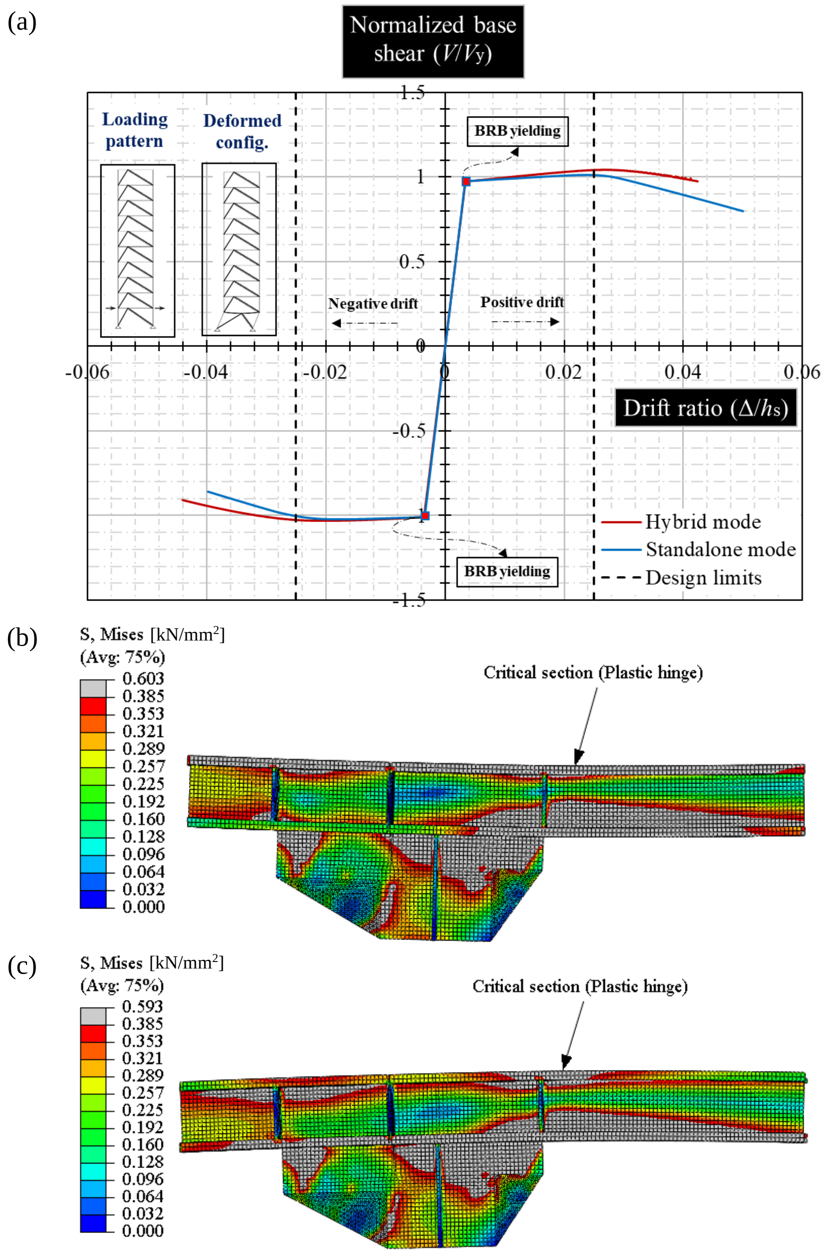

Figure 8. Pushover analysis: (a) Pushover curves, (b) von Mises stress positive drift, (c) von Mises stress negative drift.

Response history analysis

Figures 9 and 10 present the peak and residual inter-storey drift responses obtained from the dynamic nonlinear response history analysis of the E-BRBF hybrid, and the standalone models under the selected ensemble of historical records. The figures present the individual drift responses, Suites' means, as well as seismic demand curves as percentages of storey heights. The figures reveal that drift responses in both models demonstrate adequacy of the E-BRBF system in mitigating P-delta effects, where peak inter-storey drift SD curves were within the code limitation (i.e., 2.5%), and the residual post-earthquake SD drifts were within the repairable limit (i.e., <0.5%). The figures also demonstrate identical drift responses of both models (i.e., hybrid and standalone) under the tested seismic excitations (i.e., Crustal, In Slab, and Subduction Interface). These identical responses are attributed to the fact that the first storey E-BRBF beam (substructure module) remains elastic under the design level seismic excitations, as intended during design. Therefore, despite utilizing a more refined FE beam model, identical behaviour to the distributed-plasticity model is obtained for drifts within the elastic design drift range (2.5%) as further demonstrated in the pushover analysis.

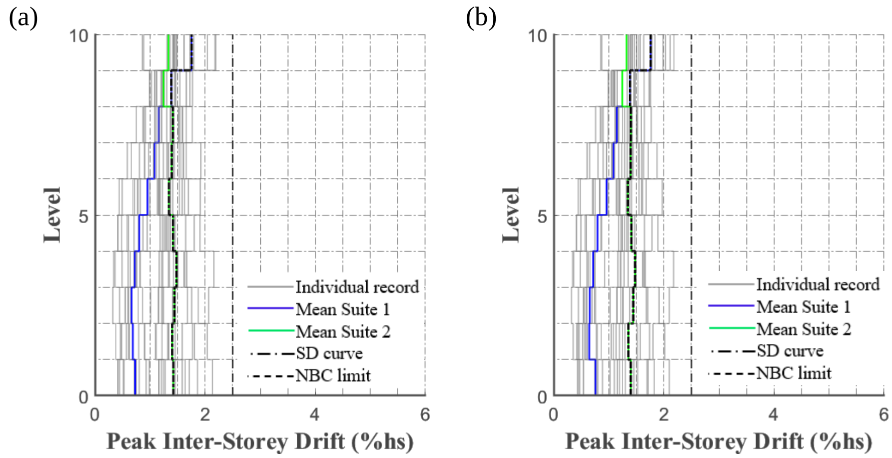

Figure 9. Peak inter-storey drift ratios, a) Standalone mode, b) Hybrid mode.

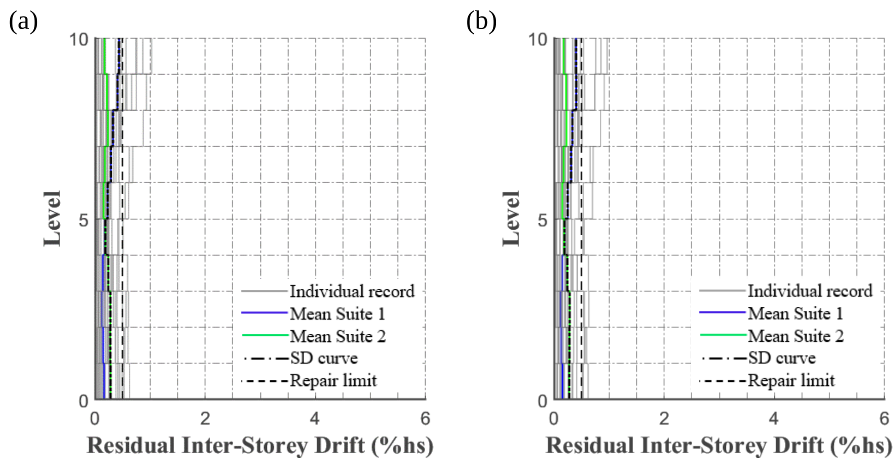

Figure 10. Residual inter-storey drift ratios: (a) Standalone mode, (b) Hybrid mode.

CONCLUSION

The global seismic stability in E-BRBFs relies heavily on the stable and predictable response of the beams under combined axial and flexural demands. This article assessed the seismic stability and the potential first-storey beam failure modes of a 10-storey E-BRBF utilizing a more refined and representative beam model using hybrid simulation. The nonlinear behaviour of the E-BRBF frame is assessed under static-monotonic analysis (pushover) and dynamic analysis (response history) using seismic excitations representative of Vancouver, BC seismic hazard (i.e., Crustal, In Slab, and Subduction Interface). The hybrid model involved a sophisticated FE model of the E-BRBF first-storey beam using Abaqus, while the rest of the E-BRBF is modelled in OpenSees using fibre-based elements. The resulting hybrid pushover curve, residual and peak inter-storey drifts were compared against their counterparts obtained using a standalone complete OpenSees model.

The dynamic response history analysis confirmed the effectiveness of the E-BRBF system in mitigating P-delta effects. The system was able to limit the peak inter-storey seismic demand drift curve within the NBC limit of 2.5% storey height, while also keeping the residual drifts within the repair limit of 0.5% storey height. When subjected to design-level scaled seismic excitations, the more refined beam model (i.e., hybrid analysis) showed identical responses to those obtained using the standalone complete OpenSees model. This confirms that the beam maintained its elastic behavior as intended in the design.

The nonlinear hybrid pushover analysis demonstrated ductile and stable behaviour of the E-BRBF beam element for a storey drift up to 4%storey height (maximum considered drift). The indicated failure mode at extreme loading involved full-plastic hinging with no instability failure. The beam in the hybrid mode demonstrated a higher contribution to global seismic stability compared to the results obtained with the standalone mode. This favourable behaviour is attributed to plastic hinges shifting beyond the extent of the gusset plate, which reduces the flexural demand on the beam and delays yielding.

ACKNOWLEDGMENTS

Financial support was provided by Fonds de recherche du Québec – Nature et technologies (FRQNT).

REFERENCES

[1] Gupta, A., and Krawinkler, H. (2000). "Dynamic P-delta effects for flexible inelastic steel structures". *Journal of Structural Engineering*, 126(1), 145-54.

[2] Williamson, E.B. (2003). "Evaluation of damage and P-δ effects for systems under earthquake excitation". *Journal of Structural Engineering*, 129(8), 1036-46.

[3] Adam, C., Ibarra, L.F. and Krawinkler, H. (2004). "Evaluation of P-delta effects in non-deteriorating MDOF structures from equivalent SDOF systems".

[4] Wei, B., Xu, Y. and Li, J. (2012). "Treatment of P-δ effects in displacement-based seismic design for SDOF systems". *Journal of Bridge Engineering*, 17(3), 509-18.

[5] Gaiotti, R., and Smith, B.S. (1989). "P-delta analysis of building structures". *Journal of Structural Engineering*, 115(4), 755-70.

[6] Merzouq, S., and Tremblay, R. (2006). "Seismic design of dual concentrically braced steel frames for stable seismic performance for multi-story buildings". In *8th US National Conference on Earthquake Engineering*.

[7] Chandramohan, R., Baker, J., Deierlein, G. and Lin, T. (2013). "Influence of ground motion spectral shape and duration on seismic collapse risk" In *10th International Conference On Urban Earthquke Engineering*, Tokyo, Japan.

[8] Raghunandan, M., Liel, A.B. and Luco, N. (2015). "Collapse risk of buildings in the pacific northwest region due to subduction earthquakes". *Earthquake Spectra*, 31(4), 2087-115.

[9] Tirca, L., Chen, L. and Tremblay, R. (2015). "Assessing collapse safety of cbf buildings subjected to crustal and subduction earthquakes". *Journal of Constructional Steel Research*, 115, 47-61.

[10] Barbosa, A.R., Ribeiro, F.L. and Neves, L.A. (2017). "Influence of earthquake ground-motion duration on damage estimation: Application to steel moment resisting frames". *Earthquake Engineering & Structural Dynamics*, 46(1), 27-49.

[11] Hariri, B., and Tremblay, R. (2023). "Optimum post-yielding stiffness design guidelines for comprehensive annihilation of seismic P-delta effects in single- and multi-storey steel buildings". Article sumbitted to *Earthquake Engineering and Structural Dynamics*.

[12] Hariri, B. and Tremblay, R. (2023). "Adequacy of secondary storey shear stiffness in annihilating the inelastic seismic p-delta effects in mid- and tall-rise steel braced frames". Article submitted to *Journal of Constructional Steel Research*.

[13] Hariri, B., and Tremblay, R. (2023). "Innovative secondary storey shear stiffness frame for seismic P-delta annihilation in tall steel buildings". Article submitted to *Journal of Constructional Steel Research*.

[14] Canadian Standard Association - CSA (2019). *CAN/CSA-S16 Design of steel structures*. Prepared by the CSA, Toronto, ON.

[15] American National Standard - ANSI (2016). ANSI/AISC-341-16 *Seismic provisions for structural steel buildings*. Prepared by the ANSI, Chicago, IL.

[16] Chen, L., Tremblay, R. and Tirca, L. (2019). "Modular tied eccentrically braced frames for improved seismic response of tall buildings". *Journal of Constructional Steel Research*, 155, 370-84.

[17] MacRae, G.A. (1994). "P-δ effects on single-degree-of-freedom structures in earthquakes". *Earthquake Spectra*, 10(3), 539-68.

[18] Jennings, P.C., and Husid, R. (1968). "Collapse of yielding structures during earthquakes". *Journal of the Engineering Mechanics Division*, 94(5), 1045-65.

[19] Tremblay, R. (2018). "An inverted V-braced frame system exhibiting bilinear response for seismic stability under long duration subduction earthquakes". In *9th International Conference on the Behaviour of Steel Structures in Seismic Areas*, Christchurch, New Zealand.

[20] Hariri, B., and Tremblay, R. (2022). "Effective steel braced frames for tall building applications in high seismic regions". In *10th International Conference On The Behaviour Of Steel Structures In Seismic Areas,* Timisoara, Romania.

[21] Huang, X., and Kwon, O.-S. (2020). "A generalized numerical/experimental distributed simulation framework". *Journal of Earthquake Engineering*, 24(4), 682-703.

[22] Mortazavi, P., Huang, X., Kwon, O. and Christopoulos, C. (2017). "Example manual for university of toronto simulation (UT-SIM) framework. An open-source framework for integrated multi-platform simulations for structural resilience". *Proc, Int Workshop on Hybrid Simulation Toronto: University of Toronto*.

[23] National Research Council of Canada NRCC (2020). NRCC/NBC National building code of canada. Prepared by NRCC, Ottawa, ON.

[24] Hariri, B., and Tremblay, R. (2021). "Influence of brace modelling on the seismic stability response of tall buckling restrained braced frame building structures". In *17th World Conference On Earthquake Engineering*, Sendai, Japan.

[25] National Research Council of Canada NRCC (2020). National building code of canada seismic hazard tool 2020 [Available from: https://earthquakescanada.nrcan.gc.ca/hazard-alea/interpolat/nbc2020-cnb2020-en.php.

[26] ABAQUS. (2022). ABAQUS Software v2022. Dassault Systemes Simulia Corporation, Providence, RI, USA.

[27] Mazzoni, S., McKenna, F., Scott, M. H. and Fenves, G. L. (2006). "Opensees command language manual". *Pacific Earthquake Engineering Research (PEER) Center*, 264.

[28] Hartloper, A.R., de Castro e Sousa, A. and Lignos, D.G. (2021). "Constitutive modeling of structural steels: Nonlinear isotropic/kinematic hardening material model and its calibration". *Journal of Structural Engineering*, 147(4).

[29] Galambos, T. V., and Ketter, R.L. (1959). "Columns under combined bending and thrust". *Journal of the Engineering Mechanics Division*, 85(2), 1-30.

[30] Zsarnóczay, Á. (2013). *Experimental and numerical investigation of buckling restrained braced frames for eurocode conform design procedure development*. Budapest University of Technology and Economics. Budapest.

[31] CoreBrace LLC. (2021). Bolted brace design guide [Available from: https://corebrace.com/wp-content/uploads/2021/04/Bolted-Connection-11-20.pdf.

[32] Hariri, B. (2023). *Innovative steel bracing systems for tall building application in high seismic regions*. Ph.D. disertation Polytechnique Montreal. Montreal, QC.

[33] Halchuk, S., Adams, J., Kolaj, M. and Allen, T. (2019). "Deaggregation of NBCC 2015 seismic hazard for selected canadian cities". In *12th Canadian Conference on Earthquake Engineering*, Quebec, QC.